

Article

Foam Stabilization by Surfactant/SiO₂ Composite Nanofluids

Fariza Amankeldi ^{1,2,*}, Miras Issakhov ^{2,*}, Peyman Pourafshary ^{2,3} , Zhanar Ospanova ^{1,2} ,
Maratbek Gabdullin ² and Reinhard Miller ⁴ 

¹ Department of Colloid, Analytical Chemistry and Technology of Rare Elements, Al-Farabi Kazakh National University, Almaty 050000, Kazakhstan; zhanar.ospanova@kaznu.kz

² School of Materials Science and Green Technology, Kazakh-British Technical University, Almaty 050000, Kazakhstan; peyman.pourafshary@nu.edu.kz (P.P.); gabdullin@physics.kz (M.G.)

³ School of Mining and Geosciences, Nazarbayev University, Astana 010000, Kazakhstan

⁴ Institute of Soft Matter Physics, Technical University of Darmstadt, 64297 Darmstadt, Germany; reinhard.miller@pkm.tu-darmstadt.de

* Correspondence: f.amankeldi@kbtu.kz (F.A.); mir001@gmail.com (M.I.); Tel.: +7-778-921-10-11 (F.A.)

Abstract: This paper deals with the potential of aggregates of surfactant and SiO₂ nanoparticles as foam stabilizers for practical applications. The effects of different chain lengths and concentrations of the cationic surfactant C_nTAB on the performance of C_nTAB–SiO₂ nanofluids are examined to gain a comprehensive understanding of their ability to stabilize foam. The results indicate enhanced foam stability in the presence of SiO₂ nanoparticles. These findings help to better understand foam stabilization and its potential in various industrial applications such as enhanced oil recovery and foam-based separation processes.

Keywords: foam stability; alkyltrimethyl ammonium bromides; silicon dioxide nanoparticles; composite foam



Citation: Amankeldi, F.; Issakhov, M.; Pourafshary, P.; Ospanova, Z.; Gabdullin, M.; Miller, R. Foam Stabilization by Surfactant/SiO₂ Composite Nanofluids. *Colloids Interfaces* **2023**, *7*, 57. <https://doi.org/10.3390/colloids7030057>

Academic Editor: Plamen Tchoukov

Received: 25 May 2023

Revised: 21 August 2023

Accepted: 27 August 2023

Published: 7 September 2023



Copyright: © 2023 by the authors. Licensee MDPI, Basel, Switzerland. This article is an open access article distributed under the terms and conditions of the Creative Commons Attribution (CC BY) license (<https://creativecommons.org/licenses/by/4.0/>).

1. Introduction

Currently, there is growing interest in composite materials that can effectively modify the practical properties of numerous types of liquid dispersal systems, which are widely used in many industries. These included foams with different quality and stability. The stability of foams can be provided by compositions of surfactants with natural and synthetic high-molecular-weight substances [1] and particles [2]. Particle-stabilized foams can be used in various industrial and technological fields, such as chemical-enhanced oil recovery, mineral flotation, and in the food industry [3–6].

Enhanced oil recovery from reservoirs is a real challenge in the global oil industry due to the decreased oil production from many reservoirs. Therefore, various efficient enhanced oil recovery (EOR) methods have been applied, including gas flooding [7–10]. Here, foam is injected and increases the apparent gas viscosity, hence reducing the gas mobility in the pores. However, the practical application of foam-based EOR shows limitations in crude oil environments caused by the rapid destabilization of foam at elevated temperatures, reducing its effectiveness.

To address these limitations and to advance the field of EOR, the present study explores new approaches to improve the stability of gas foams. Specifically, the research focuses on incorporating nanoparticles as potential foam stabilizers [9–12]. Nanoparticles possess intrinsic properties, such as chemical stability and low adsorption on mineral surfaces, which make them attractive candidates for producing highly stable foams.

Moreover, these particular properties extend their use in technology fields beyond enhanced oil recovery. Stable gas foams and emulsions have a broad range of applications, including subsurface remediation, carbon capture and storage, and even applications in the food and cosmetic industries.

This study seeks to provide valuable insights into the colloid-chemical properties of surfactant/nanoparticle mixtures in order to optimize foams with potential applications not only in the oil industry. The results will enable the design of efficient and environmentally friendly methods in many new technologies.

Nanoparticles, such as negatively charged silica particles, are attractive materials for stabilizing foam because they have a certain surface activity, which enables them to form a dense and uniform layer at the interface. Cationic surfactants are positively charged, which allows them to interact strongly with negatively charged surfaces, such as many types of nanoparticles.

One of the challenges in studying particle-stabilized foams is the complexity of phenomena that can influence their stability. These phenomena include the properties of the particles (such as size, shape, charge) [13–16], the properties of the liquid (such as viscosity and surface tension), and the environmental conditions under which the foam is formed and applied (such as shear rate, gas flow rate, and temperature) [17].

In recent years, researchers have explored the use of various types of nanoparticles, including silica, clay, and carbon-based particles [18–20]. Mixtures of silica nanoparticles and different cationic surfactants have frequently been used [21–27] to stabilize foams. These studies have provided insights into the mechanisms of foam stabilization by these materials.

Overall, the theoretical background of particle-stabilized foams using silica nanoparticles and cationic surfactants is a complex and evolving field, with many open questions still and, therefore, many opportunities for further research. The main mechanism of foam stabilization by particle/cationic surfactant mixtures is the electrostatic repulsion between the adsorbed particle layers at both sides of the foam films. These stable particle layers around the gas bubbles prevent coalescence of the foam. Also, the particles can act as a physical barrier, impeding the movement of gas bubbles and reducing the drainage of liquid from the foam. Additionally, the combination of particles and surfactant can create a synergistic effect that enhances foam stability not available by use of the surfactant alone [26,28–30].

The goal of the present work is to examine how the combination of C_n TAB–SiO₂ nanoparticles can help to stabilize foam. This understanding can lead to improved foam stability and the development of new applications for these materials. By enhancing foam stability, C_n TAB–SiO₂ mixtures may have a wide range of applications in industries such as cosmetics, food, agriculture, and EOR, where foam stability is crucial for product performance and quality.

One of the notable investigations on foam stability with surfactant–nanoparticle mixtures in foam-flooding enhanced oil recovery (EOR) is the study by Rezaei et al. [9]. In this study, it was found that the combination of the surfactant cocamido propyl betaine (CAPB) with silica nanoparticles and NaCl significantly improved foam stability, outperforming similar combinations with other surfactants, such as linear alkylbenzene sulphonic acid (LABSA) and cetyltrimethylammonium bromide (CTAB). Moreover, investigations on the effects of temperature demonstrated that CAPB exhibited superior foam stabilization up to 50 °C, after which CTAB surpassed CAPB and LABSA in stabilizing N₂ foams. These findings highlighted the potential of surfactant–nanoparticle mixtures for enhancing foam flooding as an effective method for EOR. In another study by Sun et al. [10], the use of partially hydrophobized SiO₂ nanoparticles in combination with the anionic surfactant sodium dodecyl sulfate (SDS) was shown to enhance foam stability for nitrogen foam flooding. The experimental results demonstrated that the SiO₂/SDS foam exhibited better temperature tolerance and increased surface dilational viscoelasticity, leading to the maintenance of spherical or ellipsoidal foam bubbles. The SiO₂/SDS foam also outperformed other flooding methods by effectively controlling the gas mobility, avoiding channeling, and enhancing oil recovery in micromodel and sand pack flooding experiments.

Several studies have investigated the use of cationic surfactants and silica particles to stabilize foam. For example, Wang et al. [31] investigated the interfacial rheology of nano-SiO₂ dispersions in the presence of cationic CTAB. Depending on the amount of added CTAB, the SiO₂ particles changed from hydrophilic to hydrophobic. Badri

and Pallab [32] investigated the same system and found that smaller nanoparticles were more efficient as foam stabilizers. Also, Choi et al. [33] studied the same system but used specially synthesized silica particles and confirmed previous results. Most recently, Wang [34] investigated the foaming capacity of various cationic surfactants and the effects of hydrophilic and hydrophobic SiO₂ NPs on foam stability from macroscopic and microscopic perspectives. The experimental results suggested that the concentration of nanoparticles did not significantly affect the stability of the foam; however, it was higher at elevated temperatures of 50–90 °C.

Despite the many investigations, there is not sufficient knowledge available to completely understand the underlying mechanisms to stabilize foam, particularly with respect to the effect of different alkyl chain lengths of the used cationic surfactants. Therefore, the purpose of the present work is to analyze the properties of C_nTAB–SiO₂ complexes (nanoparticles NP) as a foaming agent and to quantify the effects of both the alkyl chain length and the concentration of the used cationic surfactants.

2. Materials and Methods

2.1. Materials

Four n-alkyl trimethyl ammonium bromides (C_nH_{2n+1}(CH₃)₃N⁺Br[−]) were purchased from Sigma-Aldrich Co. (St. Louis, Missouri, USA) with a purity of >99%: decyl trimethyl ammonium bromide (C₁₀TAB), dodecyl trimethyl ammonium bromide (C₁₂TAB), tetra decyl trimethyl ammonium bromide (C₁₄TAB), and hexadecyl trimethyl ammonium bromide (C₁₆TAB).

Ludox AM-30 is an aqueous 30% colloidal suspension of SiO₂ and was purchased from Sigma-Aldrich Co. The silicon dioxide particles are nearly spherical, with an average particle size of 12 nm. The nanoparticles are negatively charged and pH stable (pH between 8.6 and 9.3) and have a specific surface area of 198–258 m²/g, as determined by BET adsorption analysis.

The 30% Ludox suspension was diluted to 3 wt% and then used to prepare mixtures with C_nTAB. The required amount of C_nTAB was dissolved in deionized water. The concentrations of the C_nTAB solutions were in the range between 10^{−5} and 10^{−1} mol/L.

The prepared C_nTAB solution was added drop-by-drop to the 3 wt% silicon dioxide particle suspension, and the mixture was stirred by a magnetic stirrer at 400 rpm for 30 min. The purpose of this step was to allow the C_nTAB to homogeneously adsorb onto the silicon dioxide particles. A 1:1 volume ratio of the C_nTAB and SiO₂ stock solutions at the given concentrations was used for the preparation of the C_nTAB–SiO₂ complexes.

2.2. Apparatus and Methods

2.2.1. Foam Generation and Stability

Foamability and foam stability measurements were carried out using the air sparging method. Gas was passed through a porous membrane at the bottom of a glass cylinder (d = 20 mm). A total of 2 mL of the sample suspension was placed in the glass cylinder, and air was injected for 15 s at a constant gas flow rate of 1.5 mL/s to generate the foam. The maximum foam height and the liquid height in the cylinder were measured immediately after terminating the foam formation.

To evaluate the foam stability, the bulk foam height was measured at different time intervals. The foam stability was determined by plotting the normalized foam height as a function of time. The normalized foam height was computed using Equation (1) as described by Yekeen et al. [35].

$$\text{Normalized foam height} \left(\frac{H}{H_0} \right) = \frac{\text{Foam height at time } t}{\text{Foam height at time } t_0} \quad (1)$$

Images of the foam were taken using a micro-camera, which was attached to the foam-generating set-up. All images were stored and subsequently analyzed.

2.2.2. Zeta Potential Measurements

The zeta potential of the nanoparticles was measured using a Zetasizer Nano ZS (Software Version 7.13) (Malvern). Before the measurements, the instrument was tested with the Malvern zeta potential transfer standard.

2.2.3. Measurement of the Surface Tension

To determine the surface tension of the suspensions, a Profile Analysis Tensiometer PAT 1M (SINTERFACE Technology, Berlin, Germany) was used. A complete description of the experimental set-up has been given in [36]. The method can measure the surface and interfacial tension of liquid/gas and liquid/liquid interfaces for periods of up to several hours and even days.

2.2.4. Image Analysis and Data Statistics

Image analysis and data statistics were performed using different software packages, such as Excel and Image J. All measurements were performed in triplicates and we calculated the mean average values and standard deviation and used error bars in the graphs.

3. Results

3.1. Foam Formation and Stability by C_n TAB–SiO₂ NPs

Figure 1 presents the maximum foam height as a function of the number of carbon atoms (n) for both pure C_n TAB and C_n TAB–SiO₂ mixtures, with the surfactant concentration fixed at 1×10^{-3} mol/L. From the figure, it is evident that the foam height was generally higher for the composite (C_n TAB–SiO₂ mixtures) compared to the pure surfactants. However, for C_{16} , the foam height was not increased by the addition of silica nanoparticles.

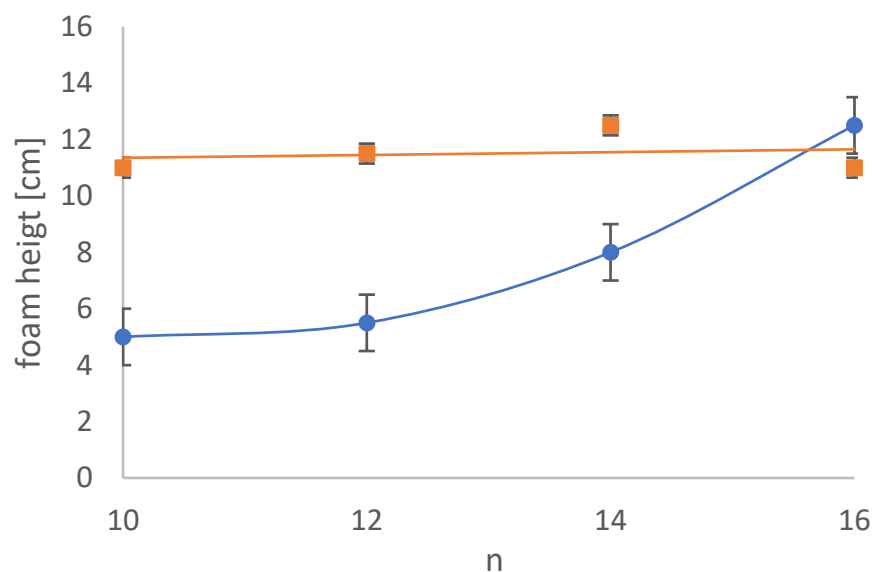


Figure 1. Maximum foam height for C_n TAB (●) and C_n TAB–SiO₂ dispersions (■) as a function of the number of carbon atoms ($n = 10, 12, 14, 16$) at a fixed surfactant concentration of 1×10^{-3} mol/L.

The foamability of dispersions of the C_n TAB–SiO₂ mixtures was investigated in a concentration range between 1×10^{-5} mol/L and 1×10^{-1} mol/L (Figure 2). It is expressed as the height of the foam produced with the dispersions after 10 min. The foamability of the mixtures varies with the concentration and chain length of C_n TAB.



Figure 2. Foamability of different C_n TAB–SiO₂ mixtures in the concentration range between 1×10^{-5} mol/L and 1×10^{-1} mol/L.

At a concentration of 1×10^{-2} mol/L, phase separation was observed for C₁₀, C₁₂, and C₁₄, which resulted in decreased foamability. An intriguing deviation in the behavior was observed for C₁₄TAB combined with SiO₂ nanoparticles, which deviated from the trends observed for C₁₀TAB, C₁₂TAB, and C₁₆TAB. At a concentration of 1×10^{-3} mol/L, the foamability of C₁₄TAB was found to be higher compared to C₁₀TAB, C₁₂TAB, and C₁₆TAB, where the foamability increased with increase in concentration. The study suggests that the foamability of C_n TAB–SiO₂ nanoparticles can be tuned by controlling the concentration and chain length of the surfactant in order to modify the nanoparticles in an optimum way to act as a foam stabilizer.

The Figures 3a,b and 4a,b show the changes in normalized foam height (H/H_0) over time at various concentrations for different surfactants, C_n TAB alone, and in mixtures with SiO₂ particles.

At a concentration of 1×10^{-3} mol/L (see Figure 3b), the foams generated from C_n TAB–SiO₂ nanoparticles behaved similarly to pure surfactant foams, but with slightly higher stability, except for C₁₆TAB, for which no significant change in the foam stability was noted. Instead, the foam remained unstable in the presence of the silica nanoparticles. In contrast, at a concentration of 1×10^{-1} mol/L (see Figure 4b), the foams generated with C₁₂TAB and C₁₄TAB exhibited high stability, while the foams generated with the C₁₀TAB and C₁₆TAB solutions showed lower stability.

These results suggest that the addition of SiO₂ NPs to C_n TAB solutions can improve foam stability, particularly for C₁₂TAB and C₁₄TAB.

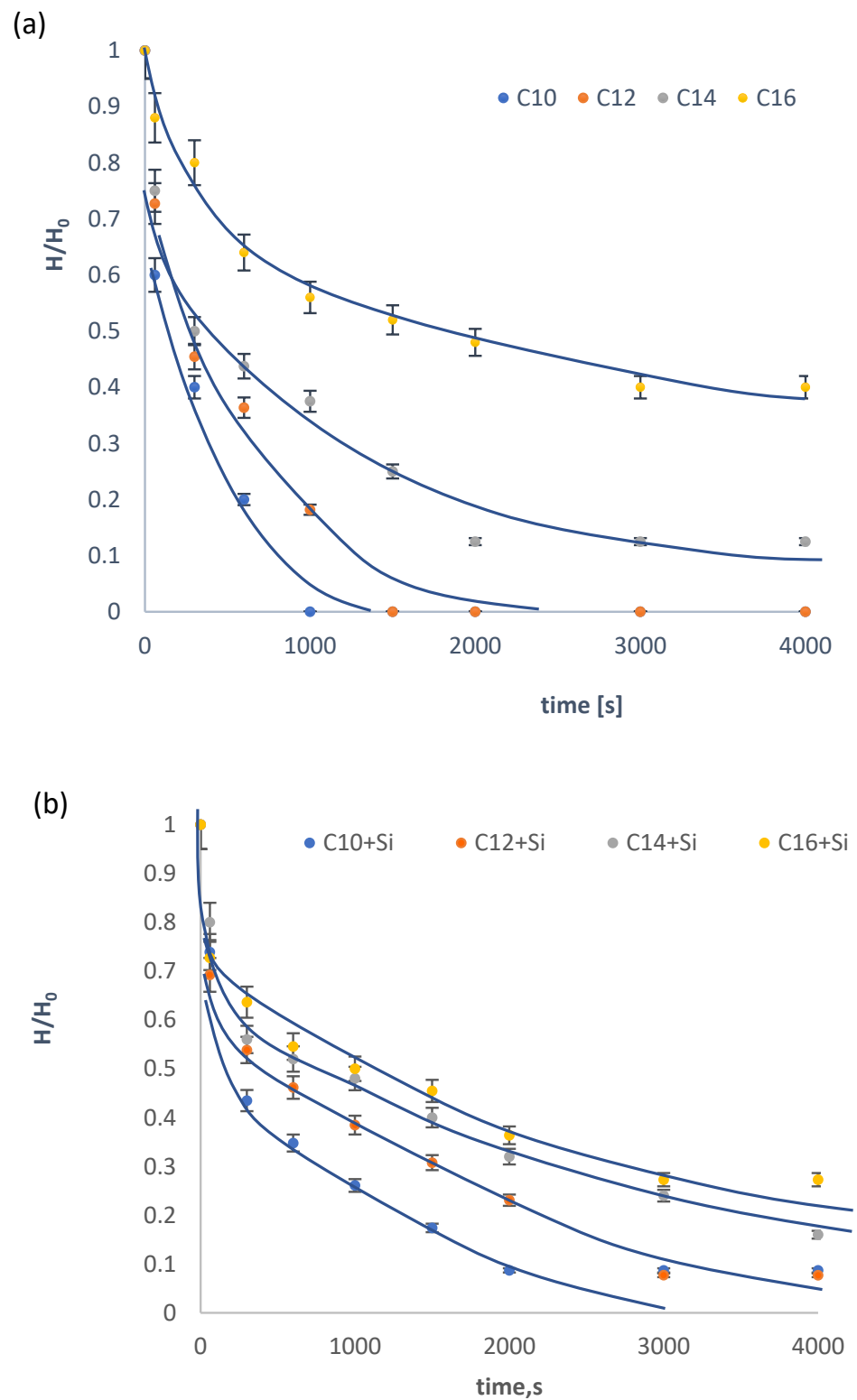


Figure 3. Normalized foam height (H/H_0) as a function of time for (a) pure C_n TAB aqueous foams and (b) C_n TAB-SiO₂ nanoparticle dispersions at a fixed surfactant concentration of 10^{-3} mol/L.

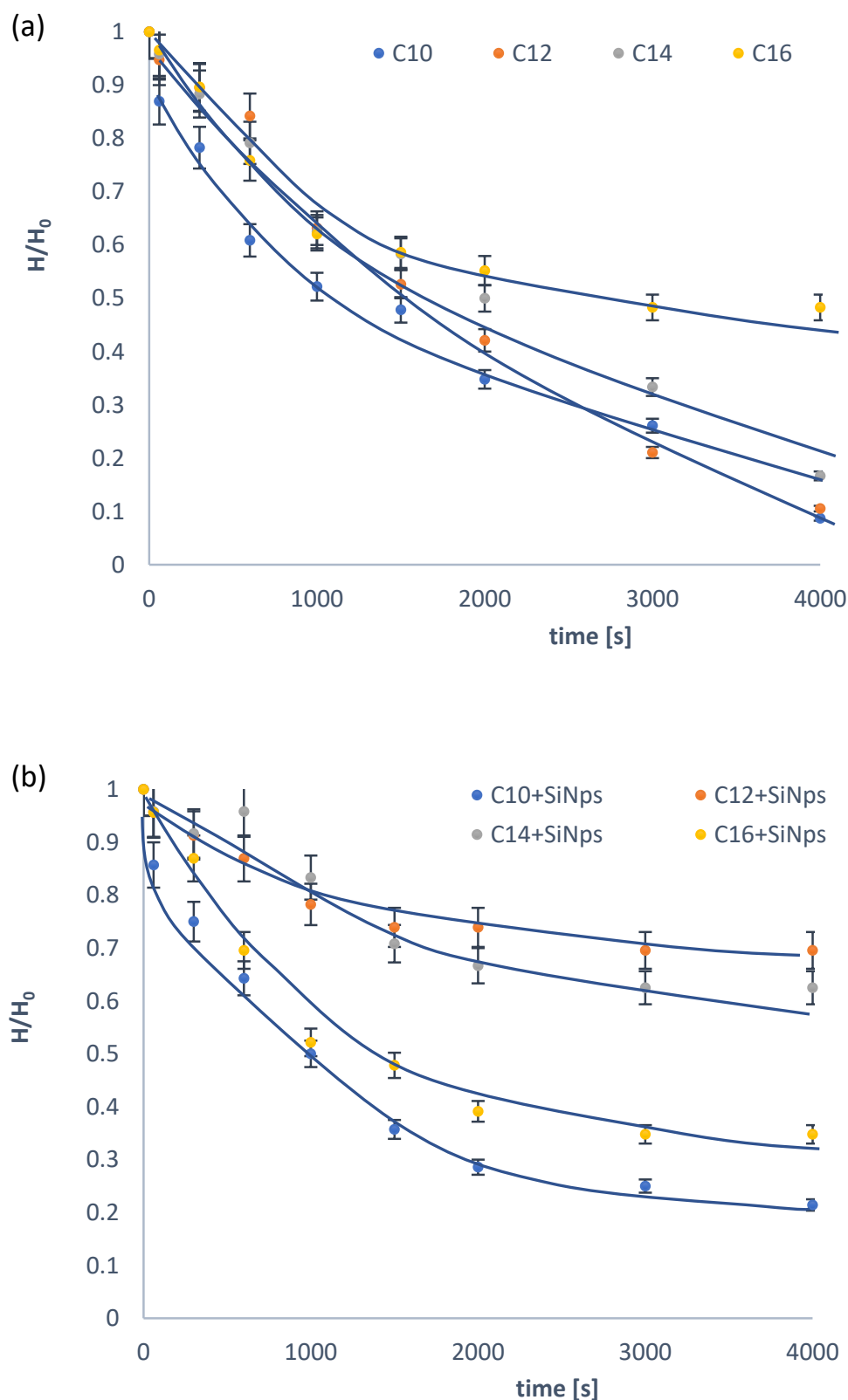


Figure 4. Normalized foam height (H/H_0) as a function of time for (a) pure C_n TAB aqueous foams and (b) C_n TAB-SiO₂ dispersions at a fixed surfactant concentration of 10^{-1} mol/L.

The foam images were taken by a microscope camera. Figure 5a shows the foam morphology for pure surfactants at a concentration of 1×10^{-3} mol/L, taken 10 min after foam formation. It was observed that, with increasing surfactant chain length, the bubble

size decreased, and the shape of the bubbles became more spherical. On the other hand, for all C_n TAB–SiO₂ mixtures (Figure 5b), the bubbles broadly appeared to be more spherical, more uniform and smaller, leading to an efficient packing density without many bubble deformations. Overall, the images provide visual evidence of the improved foam stability for C_n TAB–SiO₂ nanoparticle dispersions compared to pure surfactant solutions.

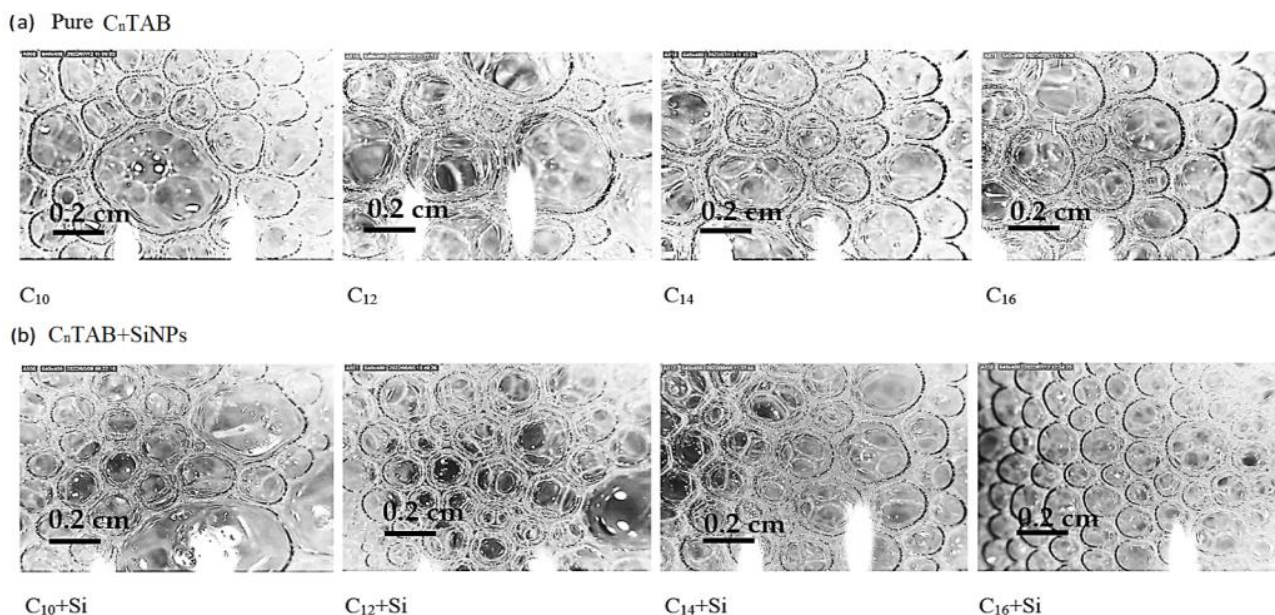


Figure 5. Morphology of foams generated with (a) pure C_n TAB and (b) C_n TAB–SiO₂ mixed solutions.

3.2. Zeta Potential of SiO₂ NPs in Aqueous Dispersions

To follow the adsorption of C_n TAB molecules onto the SiO₂ particle surfaces in the dispersion, the zeta potential of the formed particles was measured at different surfactant concentrations and using a fixed amount of 3 wt% SiO₂.

The measured zeta potentials presented in Figure 6 show how the silicon dioxide particles were step-by-step covered by the surfactants, leading to progressive surface charge compensation and further to charge inversion. Before the addition of surfactant, the silicon dioxide NPs had a zeta potential of around -38 mV, indicating a high degree of surface hydrophilicity. With increasing C_n TAB concentration, the zeta potential gradually became less negative, indicating a reduction in the surface hydrophilicity due to the adsorption of positively charged C_n TAB molecules onto the negatively charged SiO₂ particle surfaces. At a surfactant concentration above 1×10^{-2} mol/L, the zeta potential started to become positive, while the exact concentration for the charge inversion depended on the chain length. The point of zero charge indicates that the SiO₂ particles were fully covered with surfactant molecules and the surface charge had been neutralized. For C₁₄TAB and C₁₆TAB, charge neutralization began at lower surfactant concentrations, i.e., at around 10^{-2} mol/L, while for C₁₂TAB, it occurred at higher concentrations, and, for C₁₀TAB, the particle charge neutralization happened at the highest concentration of almost 10^{-1} mol/L. These differences can be attributed to the shorter alkyl chains of C₁₀TAB, resulting in a lower tendency to adsorb at the particle surface. In turn, due to the higher surfactant concentration required for a complete charge neutralization, a less efficient formation of the second corona around the particle resulted.

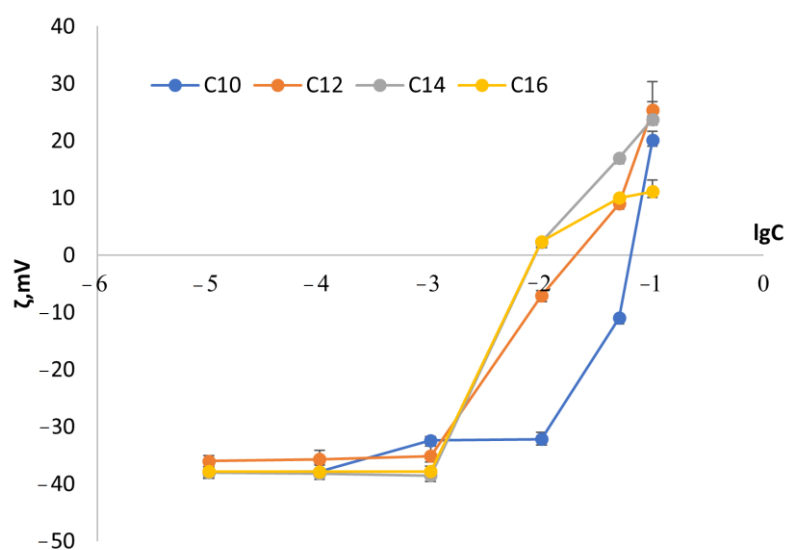


Figure 6. Zeta potential as a function of C_n TAB concentration for 3 wt% SiO_2 NP dispersions.

Additionally, as the amount of surfactant adsorbed onto the particle surface increased, the magnitude of the zeta potential also increased, becoming more and more positive until it reached values between 10 mV and 25 mV. This further confirmed the adsorption of C_n TAB onto the silicon dioxide particle surface and the formation of a bilayer structure around the SiO_2 particles.

3.3. Dynamic and Equilibrium Surface Tension of Pure C_n TAB and Mixed C_n TAB– SiO_2 Solutions

The surface tension isotherms of pure C_n TAB solutions (C_{10} , C_{12} , C_{14} , C_{16}) in Figure 7 were taken from Mucic et al. [37]. The resulting curves show a clear dependence on the chain length of the surfactant molecules, with longer chains exhibiting higher surface activity, as expected from the Traube rule. The colored experimental points are data obtained in this work, which agree rather well with the literature data in [38].

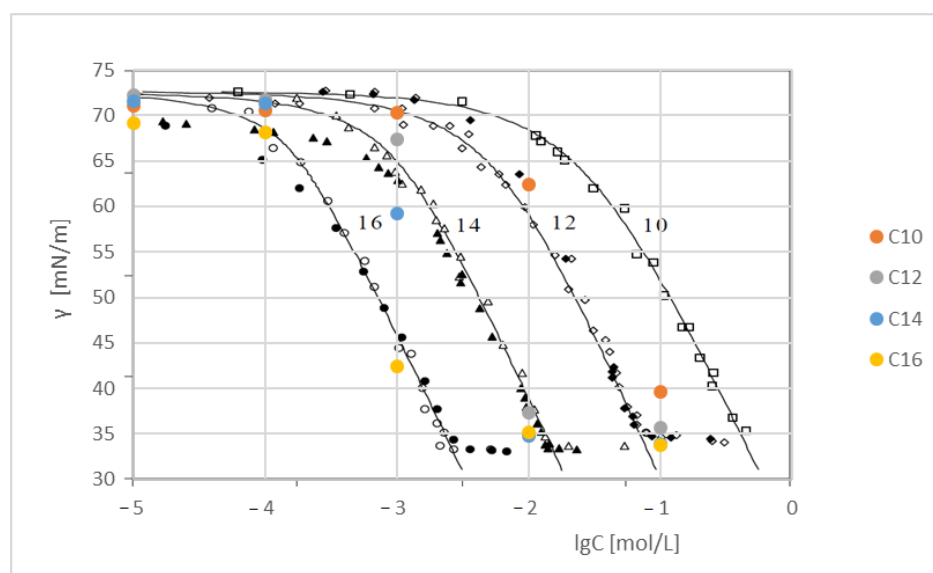


Figure 7. Surface tension isotherms of C_n TAB ($n = 10, 12, 14, 16$): colored points are actual experimental data; black symbols and curves are taken from [37].

In Figure 8, the dynamic interfacial tensions of the C_n TAB and C_n TAB– SiO_2 NP mixtures at a fixed surfactant concentration of 1×10^{-3} mol/L are shown. The results demonstrate a reduction in the surface tension for the mixture compared to the pure

surfactant solutions. All solutions of the pure C_n TABs showed an almost constant surface tension from the beginning, which means that, even after only a few seconds, the adsorption of the surfactant molecules had reached equilibrium. Due to the large differences in surface activity, the absolute values were lowest for C_{16} and highest for C_{10} TAB. In contrast, when SiO_2 particles were added to the respective surfactant solutions, the dynamic surface tension curves first decreased and then leveled off at the respective equilibrium surface tension. The much slower change in surface tension points to the fact that the surfactant molecules did not adsorb, but complex particles, i.e., the SiO_2 particles, were modified via the electrostatically bound cationic surfactants. The particles modified by the longest chains C_{16} were the most hydrophobic ones, and, hence, led to the lowest surface tension values. Aidarova et al. [39], in their study, obtained a similar result for polymers decorated by surfactants with longer hydrophobic chains, which required more time to reach a final value due to the slow diffusion of the polymer/surfactant complexes.

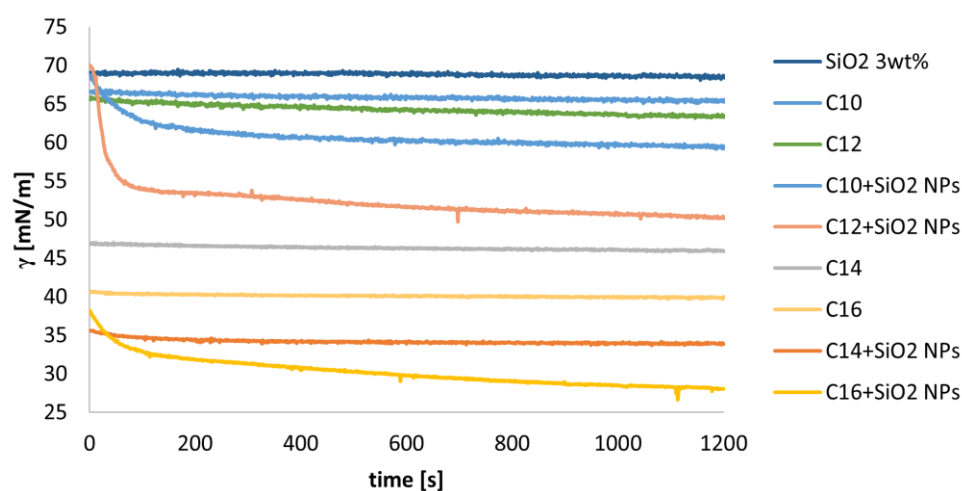


Figure 8. Dynamic surface tension $\gamma(t)$ for pure C_n TAB and C_n TAB- SiO_2 mixed solutions.

4. Discussion

4.1. C_n TAB- SiO_2 NPs Composite Foam Characteristics and Stability

Foam formation and stability are important factors in various industrial applications. The larger foamability observed in Figure 1 for the composite C_n TAB- SiO_2 as foaming agents compared to the corresponding pure surfactants (except for C_{16} TAB) can be attributed to the surfactant-silica aggregates, which were able to improve the foam stability and lead to an increased foam height.

The foamability of the mixtures varied with the concentration and chain length of C_n TAB (Figure 2). Above a concentration of 10^{-2} mol/L, the foamability for all C_n TAB- SiO_2 dispersions sharply increased. This increase in foamability was surely caused by the sufficiently high surface activity of the formed surfactant-particle complexes due to the hydrophobization effect, as well as a sufficient electric charge after the charge inversion provided by the formed second corona. Below a concentration of 10^{-2} mol/L, the complexes could possess a sufficiently high charge to stabilize the foam films and, thereby, the foam, but the corresponding surface activity was probably insufficient. The unexpected behavior of the C_{14} surfactant in combination with the SiO_2 nanoparticles presented a notable deviation from the trends observed for C_{10} TAB, C_{12} TAB, and C_{16} TAB. One plausible explanation for this particular behavior involves the concept of complete charge neutralization occurring at various surfactant concentrations, depending on the carbon chain length. Notably, shorter carbon chains require higher concentrations for achieving complete charge neutralization. At a concentration of 1×10^{-2} mol/L, it can be postulated that the particles and functional groups of C_{14} TAB experienced complete charge neutralization, contributing to the observed reduction in foamability. This observation is in line with the noticeable decrease in foamability observed above.

The results of the normalized foam height in Figures 3 and 4 indicate that the addition of SiO₂ nanoparticles to C_nTAB solutions can improve the foam stability compared to foams formed by pure surfactant solutions. The foams generated from the C_nTAB–SiO₂ mixed solutions showed a slower rate of foam decay and higher foam stability compared to the pure surfactant foams. This increased foam stability can be attributed to the presence of SiO₂ NPs in the foam films, which increased the strength of the film and reduced the rate of drainage. This was true at both the studied concentrations, 10^{−3} mol/L and 10^{−1} mol/L.

It is worth noting that the results of the study also revealed that the stability of the foams generated from the C_nTAB–SiO₂ mixtures was consistent even after particle charge neutralization, while the stability of the foams generated from the pure surfactants was reduced. This suggests that the presence of SiO₂ NPs in the foam film not only improves the initial stability during foam formation but also maintains its stability over time.

The images shown in Figure 5a,b provide additional information on the physical characteristics of the foam generated from solutions of pure surfactants and the C_nTAB–SiO₂ mixtures. The observed decrease in bubble size with increasing surfactant chain length can be attributed to the decrease in surface tension. In contrast, the C_nTAB–SiO₂ mixture foams exhibited more uniformly spherical bubbles that were densely packed. This suggests that the addition of SiO₂ NPs may act as stabilizers, helping to prevent bubble coalescence and, thereby, increasing foam stability. Additionally, the densely packed bubbles indicate that the C_nTAB–SiO₂ particles may have a higher surface coverage compared to pure surfactant foams, further supporting the idea that SiO₂ NPs can increase foam stability.

4.2. Mechanism of Foam Stabilization by C_nTAB–SiO₂ NPs

The mechanism of foam stabilization by C_nTAB–SiO₂ nanoparticles can be explained based on the results obtained for the adsorption of C_nTAB onto the surface of the colloidal silicon dioxide particles including electrostatic and hydrophobic interactions.

The change in the zeta potential of the SiO₂ NP is caused by a surface charge compensation by the adsorbed C_nTAB molecules (Figure 6). The negatively charged particle surface attracts positively charged C_nTAB molecules via electrostatic attraction. This electrostatic interaction allows the surfactant molecules to adsorb onto the silica surface, forming a primary layer. Via hydrophobic interaction, at further surfactant concentration increase, i.e., after the negative surface charges of the silica particles are compensated, the surfactant molecules adsorb at the particle surface, forming a secondary adsorption layer and causing electrostatic interparticle repulsion.

The observation that the adsorbed amounts did not differ for the studied chain lengths was not observed for C_nTAB equilibrium concentrations below 10^{−4} mol/L, which indicates that the first step of adsorption occurred before the critical micelle concentration (CMC) [37] for all C_nTABs. This suggests that the adsorption mechanism is not solely based on micelle formation, but also involves the adsorption of individual surfactant molecules onto the silica surface.

The increase in surfactant concentration gradually reduces the negative zeta potential, indicating decreased surface hydrophilicity due to the adsorption of positively charged C_nTAB molecules. Complete charge neutralization of the particles occurs at different surfactant concentrations depending on the alkyl chain length, with shorter chains requiring higher concentrations. Wu et al. (2018) [40] also observed that the affinity of silica nanoparticles to the surface can be adjusted by altering the concentration of surfactants.

The continuous increase in the zeta potential with increasing amount adsorbed of surfactants indicates that the surface of the silicon dioxide particles becomes more positively charged as more C_nTAB molecules are adsorbed. This increased positive charge on the silica surface enhances the foam stability by providing electrostatic repulsion between the bubbles.

The surface tension of pure C_nTAB solutions decreases with increasing C_nTAB concentration due to the adsorption of C_nTAB molecules at the air–water interface (Figure 7). At the same time, the maximum surface excess concentration increases with increasing chain

length. The values measured here are in good agreement with the isotherms taken from the literature [37,38].

The measured dynamic surface tension curves shown in Figure 8 are more informative than the isotherms in Figure 7 because they provide insights into the adsorption behavior of the SiO₂ NP complexes at the foam bubble surface. The dynamics of adsorption for the C_nTAB–SiO₂ systems is much slower than for the pure C_nTAB solutions at the same surfactant concentration. The slower rate of adsorption is clearly caused by the larger size of the surfactant–particle aggregates and their lower concentration compared to the pure molar surfactant solutions.

Interestingly, in Figure 8, the C₁₆TAB–SiO₂ system exhibits the lowest dynamic surface tension, suggesting efficient surfactant impact on the reduction in the surface tension at the air–water interface. However, the foam stability of the system appears to be relatively low. This observation can be attributed to the effect of silica nanoparticles on the foam behavior. Previous studies have shown that the presence of nanoparticles at the interface can even hinder the formation of a stable foam structure [41]. Silica nanoparticles tend to adsorb at the interface and may limit the mobility and arrangement of surfactant molecules, affecting their ability to form a cohesive surfactant film around the gas bubbles. Additionally, the hydrophobicity of the nanoparticles can play a significant role, with highly hydrophobic nanoparticles potentially causing agglomeration at the interface and contributing to foam destabilization.

The general behavior of C_nTAB–SiO₂ interaction and its impact on foam stabilization can be explained based on the cartoon provided in Figure 9. The interaction between C_nTAB and SiO₂ nanoparticles plays a crucial role in foam stabilization. This figure illustrates the behavior of two SiO₂ particles in a position of interacting with each other at different stages of surfactant molecules adsorbing at their surface, shedding light on the underlying mechanisms.

In the absence of surfactants (Figure 9a), the SiO₂ particles experience repulsion due to their negative surface charge, resulting in a well-dispersed suspension. The repulsion is primarily governed by electrostatic forces between the charged particles, while the van der Waals forces, which are typically weak at this stage, play a minor role [42]. However, as the surfactant concentration increases, the first layer of C_nTAB molecules adsorbs onto the surface of the SiO₂ particles (Figure 9b). This adsorption process generates a hydrophobic attraction between the particles. The hydrophobic tails of the surfactant molecules interact with each other, leading to flocculation or agglomeration of the SiO₂ particles. Additionally, van der Waals forces can also contribute to the particle flocculation at this stage. At surfactant concentrations above this point of zero charge (i.e., the concentration at which the surfaces of SiO₂ particles are neutralized), bilayer adsorption occurs (Figure 9c). This process results in the generation of positive charges at the surface of the SiO₂ particles. The electrostatic repulsion between the positively charged particles counteracts the hydrophobic attraction, thereby redispersing the suspension once again.

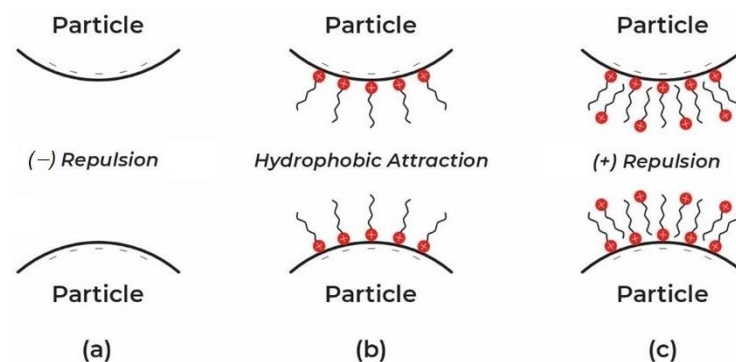


Figure 9. Microcosmic behavior of two silica particles during different stages of surfactant adsorption: (a) without any adsorption; (b) monolayer adsorption; (c) bilayer adsorption, according to [43].

These microcosmic interactions between the C_n TAB and SiO_2 nanoparticles highlight the complex interplay between electrostatic and hydrophobic forces, resulting in the stabilization or destabilization of the foam. The flocculation and subsequent dispersion of the SiO_2 particles can have direct implications for foam stabilization, as the interaction behavior of the particles affects foam structure, drainage, and stability.

5. Conclusions

In this study, we investigated the stabilization of aqueous foam by C_n TAB– SiO_2 complexes. The results provide insights into the interfacial properties and interactions within the nanofluid system that are essential for explaining the mechanisms governing the formation and stabilization of foam.

The tests performed confirm the higher foam stability caused by the presence of C_n TAB– SiO_2 complexes compared to the effects provided by pure surfactants. The foam height, drainage rate, and bubble size distribution measurements consistently support the improved foam stability in the presence of the modified SiO_2 nanoparticles.

The dynamic surface tension measurements undertaken reveal a significant reduction in surface tension for the C_n TAB– SiO_2 nanofluid systems compared to the pure surfactant solutions, indicating an interaction between the surfactant and SiO_2 nanoparticles, leading to sufficiently high surface activity required for high foamability and foam stability.

First and foremost, the improved foam stability achieved via the C_n TAB– SiO_2 complexes has profound implications for enhanced oil recovery strategies. These stabilized foams can potentially enhance oil displacement and recovery rates, thereby contributing to the optimization of oil production processes. Furthermore, the enhanced foam stability has broader applications in foam-based separation processes and mineral flotation, where stable foams play an essential role in achieving the efficient separation and concentration of valuable materials. Additionally, the novel insights into the interfacial behavior of C_n TAB– SiO_2 nanofluids provided have implications for designing advanced materials and formulations for various industries, including subsurface remediation and CO_2 capture and storage.

Author Contributions: Investigation, writing—original draft preparation F.A. and M.I.; writing—review and editing P.P., Z.O. and R.M.; supervision Z.O., R.M. and M.G. All authors have read and agreed to the published version of the manuscript.

Funding: This research was funded by Ministry of Science and Higher Education of the Republic of Kazakhstan, grant number IRN AP14869372.

Data Availability Statement: Mendeley Data, V1, doi: 10.17632/sfbppnjy7r.1.

Acknowledgments: We would like to express our sincere gratitude to S. Aidarova and P. Takhistov for their invaluable guidance and support throughout the research process.

Conflicts of Interest: The authors declare no conflict of interest.

References

1. Lindman, B.; Antunes, F.; Aidarova, S.; Miguel, M.; Nylander, T. Polyelectrolyte-surfactant association—From fundamentals to applications. *Colloid J.* **2014**, *76*, 585–594. [[CrossRef](#)]
2. Amani, P.; Miller, R.; Javadi, A.; Firouzi, M. Pickering foams and parameters influencing their characteristics. *Adv. Colloid Interface Sci.* **2022**, *301*, 102606. [[CrossRef](#)] [[PubMed](#)]
3. Yang, W.; Wang, T.; Fan, Z.; Miao, Q.; Deng, Z.; Zhu, Y. Foams stabilized by in situ-modified nanoparticles and anionic surfactants for enhanced oil recovery. *Energy Fuel* **2017**, *31*, 4721. [[CrossRef](#)]
4. Farrokhpay, S. The significance of froth stability in mineral flotation. *Adv. Colloid Interface Sci.* **2011**, *166*, 7. [[CrossRef](#)]
5. Guo, F.; Aryana, S. An experimental investigation of nanoparticle-stabilized CO_2 foam used in enhanced oil recovery. *Fuel* **2016**, *186*, 42. [[CrossRef](#)]
6. Dickinson, E. Food emulsions and foams: Stabilization by particles. *Curr. Opin. Colloid Interface Sci.* **2010**, *15*, 40–49. [[CrossRef](#)]
7. Fakoya, M.F.; Shah, S.N. Emergence of nanotechnology in the oil and gas industry: Emphasis on the application of silica nanoparticles. *Petroleum* **2017**, *3*, 391–405. [[CrossRef](#)]
8. Wang, G.; Wang, K.; Lu, C.; Wang, Y. Preparation and foam properties of Janus particles. *Chem. J. Chin. Univ.* **2018**, *39*, 990–995.

9. Rezaei, A.; Derikvand, Z.; Parsaei, F.; Imanivarnosfaderani, M. Surfactant-silica nanoparticle stabilized N-2-foam flooding: A mechanistic study on the effect of surfactant type and temperature. *J. Mol. Liq.* **2020**, *325*, 115091. [[CrossRef](#)]
10. Sun, Q.; Li, Z.; Li, S.; Jiang, L.; Wang, J.; Wang, P. Utilization of surfactant-stabilized foam for enhanced oil recovery by adding nanoparticles. *Energy Fuels* **2014**, *28*, 2384–2394. [[CrossRef](#)]
11. Almahfood, M.; Bai, B. The synergistic effects of nanoparticle-surfactant nanofluids in EOR applications. *J. Pet. Sci. Eng.* **2018**, *171*, 196–210. [[CrossRef](#)]
12. Wasan, D.T.; Nikolov, A.D. Spreading of nanofluids on solids. *Nature* **2003**, *423*, 156. [[CrossRef](#)] [[PubMed](#)]
13. Stocco, A.; Drenckhan, W.; Rio, E.; Langevin, D.; Binks, B.P. Particle-stabilised foams: An interfacial study. *Soft Matter* **2009**, *5*, 2215–2222. [[CrossRef](#)]
14. Dickinson, E.; Ettelaie, R.; Kostakis, T.; Murray, B. Factors controlling the formation and stability of air bubbles stabilized by partially hydrophobic silica nanoparticles. *Langmuir* **2004**, *20*, 8517–8525. [[CrossRef](#)]
15. Kim, I.; Worthen, A.J.; Johnston, K.P.; Di Carlo, D.A.; Huh, C. Size-dependent properties of silica nanoparticles for Pickering stabilization of emulsions and foams. *J. Nanopart. Res.* **2016**, *18*, 82. [[CrossRef](#)]
16. Fameau, A.L.; Salonen, A. Effect of particles and aggregated structures on the foam stability and aging. *C. R. Phys.* **2014**, *15*, 748–760. [[CrossRef](#)]
17. Maestro, A.; Rio, E.; Drenckhan, W.; Langevin, D.; Salonen, A. Foams stabilized by mixtures of nanoparticles and oppositely charged surfactants: Relationship between bubble shrinkage and foam coarsening. *Soft Matter* **2014**, *10*, 6975–6983. [[CrossRef](#)]
18. Zhu, Y.; Jiang, J.-Z.; Cui, Z.-G.; Binks, B.P. Responsive Aqueous Foams Stabilized by Silica Nanoparticles Hydrophobized in situ with a Switchable Surfactant. *Soft Matter* **2014**, *10*, 9739–9745. [[CrossRef](#)]
19. Verma, A.; Chauhan, G.; Ojha, K. Synergistic effects of polymer and bentonite clay on rheology and thermal stability of foam fluid developed for hydraulic fracturing. *Asia-Pac. J. Chem. Eng.* **2017**, *12*, 872–883. [[CrossRef](#)]
20. Santini, E.; Ravera, F.; Ferrari, M.; Alfè, M.; Ciajolo, A.; Liggieri, L. Interfacial properties of carbon particulate-laden liquid interfaces and stability of related foams and emulsions. *Colloids Surf. A Physicochem. Eng. Asp.* **2010**, *365*, 189–198. [[CrossRef](#)]
21. Vatanparast, H.; Javadi, A.; Bahramian, A. Silica nanoparticles cationic surfactants interaction in water-oil system. *Colloids Surfaces A Physicochem. Eng. Asp.* **2017**, *521*, 221–230. [[CrossRef](#)]
22. Liggieri, L.; Santini, E.; Guzman, E.; Maestro, A.; Ravera, F. Wide-frequency dilational rheology investigation of mixed silica nanoparticle—CTAB interfacial layers. *Soft Matter* **2011**, *7*, 7699–7709. [[CrossRef](#)]
23. Calzolari, D.C.E.; Pontoni, D.; Deutsch, M.; Reichert, H.; Daillant, J. Nanoscale structure of surfactant-induced nanoparticle monolayers at the oil—Water interface. *Soft Matter* **2012**, *8*, 11478–11483. [[CrossRef](#)]
24. Wang, W.; Gu, B.; Liang, L.; Hamilton, W.A. Adsorption and Structural Arrangement of Cetyltrimethylammonium Cations at the Silica Nanoparticle-Water Interface. *J. Phys. Chem. B* **2004**, *108*, 17477–17483. [[CrossRef](#)]
25. Cui, Z.; Yang, L.; Cui, Y.; Binks, B.P. Effects of Surfactant Structure on the Phase Inversion of Emulsions Stabilized by Mixtures of Silica Nanoparticles and Cationic Surfactant. *Langmuir* **2010**, *26*, 4717–4724. [[CrossRef](#)] [[PubMed](#)]
26. Santini, E.; Krägel, J.; Ravera, F.; Liggieri, L.; Miller, R. Study of the monolayer structure and wettability properties of silica nanoparticles and CTAB using the Langmuir trough technique. *Colloids Surf. A Physicochem. Eng. Asp.* **2011**, *382*, 186–191. [[CrossRef](#)]
27. Stamkulov, N.; Mussabekov, K.; Aidarova, S.; Luckham, P. Stabilization of emulsions by using a combination of an oil soluble ionic surfactant and water-soluble polyelectrolytes. I: Emulsion stabilization and Interfacial tension measurements. *Colloids Surf. A Physicochem. Eng. Asp.* **2009**, *335*, 103–106. [[CrossRef](#)]
28. Eskandar, N.G.; Simovic, S.; Prestidge, C.A. Synergistic effect of silica nanoparticles and charged surfactants in the formation and stability of submicron oil-in-water emulsions. *Phys. Chem. Chem. Phys.* **2007**, *9*, 6426–6434. [[CrossRef](#)] [[PubMed](#)]
29. Binks, B.P.; Desforges, A.; Duff, D.G. Synergistic stabilization of emulsions by a mixture of surface-active nanoparticles and surfactant. *Langmuir* **2007**, *23*, 1098–1106. [[CrossRef](#)] [[PubMed](#)]
30. Binks, B.P.; Rodrigues, J.A.; Frith, W.J. Synergistic interaction in emulsions stabilized by a mixture of silica nanoparticles and cationic surfactant. *Langmuir* **2007**, *23*, 3626–3636. [[CrossRef](#)]
31. Wang, H.; Gong, Y.; Lu, W.; Chen, B. Influence of nano-SiO₂ on dilational viscoelasticity of liquid/air interface of cetyltrimethyl ammonium bromide. *Appl. Surf. Sci.* **2008**, *254*, 3380–3384. [[CrossRef](#)]
32. Badri, V.; Pallab, G. The effect of silica nanoparticles on the stability of aqueous foams. *J. Dispers. Sci. Technol.* **2019**, *40*, 206–218.
33. Choi, M.; Kim, S.E.; Yoon, I.H.; Jung, C.H.; Choi, W.K.; Moon, J.K.; Kim, S.B. Effect of cetyltrimethyl ammonium bromide on foam stability and SiO₂ separation for decontamination foam application. *J. Nucl. Fuel Cycle Waste Technol.* **2018**, *16*, 173–182. [[CrossRef](#)]
34. Wang, X.; Xu, P.; Xu, M.; Pu, L.; Zhang, Y. Synergistic improvement of foam stability with SiO₂ nanoparticles (SiO₂-NPs) and different surfactants. *Arab. J. Chem.* **2023**, *16*, 104394.
35. Yekeen, N.; Idris, A.K.; Manan, M.A.; Samin, A.M. Experimental study of the influence of silica nanoparticles on the bulk stability of SDS-foam in the presence of oil. *J. Dispersion Sci. Technol.* **2017**, *38*, 416–424. [[CrossRef](#)]
36. Zholob, S.A.; Makievski, A.V.; Miller, R.; Fainerman, V.B. Optimization of calculation methods for determination of surface tensions by drop profile analysis tensiometry. *Adv. Colloid Interface Sci.* **2007**, *134–135*, 322–329. [[CrossRef](#)]
37. Mucic, N.; Moradi, N.; Javadi, A.; Aksenenko, E.V.; Fainerman, V.B.; Miller, R. Mixed adsorption layers at the aqueous C_nTAB solution/hexane vapour interface. *Colloids Surf. A Physicochem. Eng. Asp.* **2014**, *442*, 50–55. [[CrossRef](#)]

38. Mukerjee, P.; Mysels, K.J. *Critical Micelle Concentrations of Aqueous Surfactant Systems*; National Bureau of Standards: U.S. Government Printing Office: Washington, DC, USA, 1971; pp. 104–107.
39. Aidarova, S.; Sharipova, A.; Krägel, J.; Miller, R. Polyelectrolyte/surfactant mixtures in the bulk and at water/oil interfaces. *Adv. Colloid Interface Sci.* **2014**, *205*, 87–93. [[CrossRef](#)]
40. Wu, Y.; Fang, S.; Zhang, K.; Zhao, M.; Jiao, B.; Dai, C. The stability mechanism of nitrogen foam in porous media with silica nanoparticles modified by cationic surfactants. *Langmuir* **2018**, *34*, 8015–8023. [[CrossRef](#)]
41. Zargartalebi, M.; Kharrat, R.; Barati, N. Enhancement of surfactant flooding performance by the use of silica nanoparticles. *Fuel* **2015**, *143*, 21–27. [[CrossRef](#)]
42. Vincent, B. Early (pre-DLVO) studies of particle aggregation. *Adv. Colloid Interface Sci.* **2012**, *170*, 56–67. [[CrossRef](#)] [[PubMed](#)]
43. Miller, R.; Alahverdijeva, V.S.; Fainerman, V.B. Thermodynamics and rheology of mixed protein-surfactant adsorption layers. *Soft Matter* **2008**, *4*, 1141–1146. [[CrossRef](#)] [[PubMed](#)]

Disclaimer/Publisher's Note: The statements, opinions and data contained in all publications are solely those of the individual author(s) and contributor(s) and not of MDPI and/or the editor(s). MDPI and/or the editor(s) disclaim responsibility for any injury to people or property resulting from any ideas, methods, instructions or products referred to in the content.